



ELSEVIER



## Safety of the intravenous administration of neurotensin-polyplex nanoparticles in BALB/c mice

Maria E. Hernandez, PhD<sup>a</sup>, Jesus D. Rembao, MD, PhD<sup>b</sup>, Daniel Hernandez-Baltazar, PhD<sup>f</sup>, Rosa A. Castillo-Rodriguez, MSc<sup>f</sup>, Victor M. Tellez-Lopez, MSc<sup>f</sup>, Yazmin M. Flores-Martinez, MSc<sup>f</sup>, Carlos E. Orozco-Barrios, PhD<sup>f</sup>, Hector A. Rubio, MD, PhD<sup>c</sup>, Aurora Sánchez-García, BSc<sup>b</sup>, Jose Ayala-Davila, BSc<sup>f</sup>, Martha L. Arango-Rodriguez, PhD<sup>d</sup>, Lenin Pavón, PhD<sup>a</sup>, Teresa Mejia-Castillo, PhD<sup>f</sup>, Patricia Forgez, PhD<sup>e</sup>, Daniel Martinez-Fong, MD, PhD<sup>f,g,\*</sup>

<sup>a</sup>Department of Psychoimmunology, INPRF, Mexico DF, Mexico

<sup>b</sup>Department of Neuropathology, INNN, Mexico DF, Mexico

<sup>c</sup>School of Medicine, UADY, Merida, Yucatan, Mexico

<sup>d</sup>Instituto de Ciencias, Facultad de Medicina Clínica Alemana Universidad del Desarrollo, Santiago, Chile

<sup>e</sup>UMR\_S938, Hôpital Saint-Antoine, Paris Cedex 12, France

<sup>f</sup>Department of Physiology, Biophysics and Neurosciences, CINVESTAV-I.P.N., Mexico DF, Mexico

<sup>g</sup>PhD Program in Nanoscience and Nanotechnology; CINVESTAV-I.P.N., Mexico DF, Mexico

Received 16 July 2013; accepted 20 November 2013

### Abstract

Neurotensin (NTS)-polyplex is a gene nanocarrier that has potential nanomedicine-based applications for the treatment of Parkinson's disease and cancers of cells expressing NTS receptor type 1. We assessed the acute inflammatory response to NTS-polyplex carrying a reporter gene in BALB/c mice. The intravenous injection of NTS-polyplex caused the specific expression of the reporter gene in gastrointestinal cells. Six hours after an intravenous injection of propidium iodide labeled-NTS-polyplex, fluorescent spots were located in the cells of the organs with a mononuclear phagocyte system, suggesting NTS-polyplex clearance. In contrast to lipopolysaccharide and carbon tetrachloride, NTS-polyplex did not increase the serum levels of tumor necrosis factor alpha, interleukin (IL)-1 $\beta$ , IL-6, bilirubin, aspartate transaminase, and alanine transaminase. NTS-polyplex increased the levels of serum amyloid A and alkaline phosphatase, but these levels normalized after 24 h. Compared to carrageenan, the local injection of NTS-polyplex did not produce inflammation. Our results support the safety of NTS-polyplex.

**From the Clinical Editor:** This study focuses on the safety of neurotensin (NTS)-polyplex, a gene nanocarrier that has potential in the treatment of Parkinson's disease and cancers of cells expressing NTS receptor type 1. NTS polyplex demonstrates a better safety profile compared with carrageenan, lipopolysaccharide, and carbon tetrachloride in a murine model.

© 2014 Elsevier Inc. All rights reserved.

**Key words:** Nanomaterials; Pro-inflammatory cytokines; Biosafety; Cytotoxicity

Sources of Support: This research was supported by ANR-CONACYT Grant # 142947.

Financial Disclosure: The authors have no financial, personal or other relationships with other people or organizations within five years of the beginning of the submitted work that could inappropriately influence, or be perceived to influence, their work. The authors declared that no competing interests exist.

\*Corresponding author at: Departamento de Fisiología, Biofísica y Neurociencias, CINVESTAV, Apartado postal 14-740, México D.F., 07000 México.

E-mail addresses: [dmartine@fisio.cinvestav.mx](mailto:dmartine@fisio.cinvestav.mx), [martinez.fong@gmail.com](mailto:martinez.fong@gmail.com) (D. Martinez-Fong).

1549-9634/\$ – see front matter © 2014 Elsevier Inc. All rights reserved.  
<http://dx.doi.org/10.1016/j.nano.2013.11.013>

Neurotensin (NTS)-polyplex is a nanocarrier that enables the delivery of genetic material to cells that express and internalize the NTS receptor type 1 (NTSR1), including dopamine neurons and cancer cells.<sup>1-5</sup> The NTS-polyplex consists of toroidal nanoparticles (NPs) (average diameter 150 nm) that result from the compaction of a plasmid DNA (pDNA) via the electrostatic binding of the Vp1 SV40 karyophilic peptide (KP) and the NTS-carrier, which is a conjugate of poly-L-lysine, NTS, and the hemagglutinin-derived HA2 fusogenic peptide (FP).<sup>6</sup> The NTS-carrier promotes gene entry via NTSR1 internalization.<sup>1-5</sup> The FP rescues the NTS-polyplex NPs from acidic endosomes, and the KP targets the pDNA to the cell nucleus, which enhances transfection

efficiency.<sup>4,7</sup> The inclusion of a tissue-specific gene promoter provides a second point of selectivity to the NTS-polyplex NPs and drives a long-lasting transgene expression in experimental animals.<sup>6,8</sup> To date, the NTS-polyplex NPs have been used to develop two nanomedicine-based treatments that exert two opposite effects depending on the cell type of interest for transfection and the type of transgene delivered. In a therapy for Parkinson's disease, NTS-polyplex NPs deliver a neurotrophic gene into the surviving dopamine neurons of the substantia nigra known to express the highest density of NTSR1.<sup>9,10</sup> A single dose of locally injected NTS-polyplex NPs leads to the sustained expression of the neurotrophic gene and effectively functionally restores the nigrostriatal system in the rat.<sup>7,8</sup> In anticancer therapy, NTS-polyplex NPs are used to deliver a suicide gene into cancer cells that overexpress or *de novo* express NTSR1 because of transcriptional deregulation in the Wnt/beta-catenin pathway.<sup>11–13</sup> As recently shown in animal models of neuroblastoma and human breast cancer,<sup>14,15</sup> this approach is designed to specifically promote the apoptosis of tumor cells via the expression of the suicide gene and complementary pro-drug treatment. In suicide gene therapy, a single dose of intravenously injected NTS-polyplex NPs can express the transgene; however, four doses of NTS-polyplex administered every two days are necessary to significantly reduce tumor growth in an athymic mouse model of neuroblastoma<sup>14</sup> and breast cancer.<sup>15</sup>

The administration of gene nanocarriers through the bloodstream causes various interactions with the blood components.<sup>16,17</sup> One of the first interactions is the binding of the nanocarrier with proteins and erythrocytes, which rapidly forms aggregates that can be toxic due to the embolization of the particles in the lungs.<sup>18–20</sup> Proteins adsorbed on the surface of the nanocarriers also promote opsonization, which leads to aggregation and clearance from the bloodstream.<sup>17,21,22</sup> An excessive accumulation of NTS-polyplex NPs might occur in organs involved in clearance and filtration or in tissues that constitutively express NTSR1, such as the gastrointestinal tract.<sup>14,23,24</sup>

Neutrophils and macrophages are the first cells of the innate immune system that recognize, ingest, and destroy the foreign nanocarrier.<sup>25</sup> During these processes, phagocytic cells secrete several reactive oxygen intermediates and pro-inflammatory cytokines, such as tumor necrosis factor alpha (TNF- $\alpha$ ).<sup>26</sup> In addition, the liver releases complementary factors and acute phase proteins that contribute to the nanomaterial-induced inflammatory response.<sup>27,28</sup> In this regard, polyplexes have a low toxicity and weak influence on the innate immune responses<sup>26</sup> in comparison to lipoplexes and viral gene vectors.<sup>29,30</sup> To date, the safety of NTS-polyplex NPs administration has not yet been evaluated. Because NTS-polyplex NPs have been used at the same dose and the functionality of that dose has been assessed differently in different animal models, the objective of this study was to first determine whether an effective dose of NTS-polyplex NPs carrying an innocuous gene might cause cytotoxicity and acute inflammation. This study was carried out in BALB/c mice without xenografts of cancer cells or a 6-hydroxydopamine lesion of the nigrostriatal system to rule out the inflammatory response associated with the experimental procedure that generates the disease model. Carbon tetrachloride (CCl<sub>4</sub>) and lipopolysaccharide (LPS) administration was used to

compare the effects of an intravenous injection of NTS-polyplex NPs. In addition, the effects of NTS-polyplex NPs injected into the paw of BALB/c mice (a model of local inflammation) were compared with carrageenan (Cg)-induced acute inflammation.

## Methods

### *Synthesis of the NTS-carrier and NTS-polyplex NPs formation*

The NTS-carrier synthesis and NTS-polyplex NPs formation at an optimum molar ratio have been previously reported.<sup>2,6</sup> NTS (Sigma-Aldrich; Saint Louis, MO, USA) and a modified hemagglutinin-HA2 FP (GLFEAIAEFIEGGWEGLIEGCAKKK; purity >90%; RS Synthesis; Louisville, KY, USA) were cross-linked with poly-L-lysine (48 kDa mean molecular mass; Sigma-Aldrich; Saint Louis, MO, USA) using LC-SPDP (Thermo Scientific Pierce; Rockford, IL, USA).<sup>2</sup> Gel-filtration chromatography was used to purify the SPDP-derivatives and the NTS-SPDP-(FP-SPDP)-poly-L-lysine conjugate (NTS-carrier). To form the NTS-polyplex NPs, the NTS-carrier and the mutant Vp1-SV40 KP (MAPTKRKGSCPGAAPNPKPK; 90% purity; RS Synthesis; Louisville, KY, USA) were electrostatically bound to pEGFP-N1, a plasmid coding for the enhanced green fluorescent protein (GFP; 4,733 bp; Clontech, Palo Alto, CA, USA), as previously described.<sup>2,4,6</sup> Retention and retardation microassays<sup>2,4,6</sup> were used to determine the optimum molar ratio of polyplex components, which was 30 nM pEGFP-N1:30  $\mu$ M KP:630 nM NTS-carrier. This molar ratio effectively results in the expression of reporter and therapeutic genes in nigral dopaminergic neurons of normal<sup>4,6</sup> and Parkinsonian rats<sup>7,8</sup> as well as in cancer cells xenografted in athymic mice.<sup>14,15</sup> At this molar ratio, the concentration of NTS is 630 nm as determined by <sup>125</sup>I-NTS.<sup>6</sup> Based on the concentration of NTS in 300  $\mu$ L (injection volume), the dose of NTS-polyplex was 8.5 nmol/kg of body weight.

### *Scanning electron microscopy*

Samples of NTS-polyplex NPs prepared in DMEM at the optimal molar ratio were placed on a specimen stub (aluminum-iron) stuck to a double-sided adhesive tape # 5085 SPI-AB-Cu. The samples were then dried in a vacuum chamber (Secador™ 1.0 Desiccator cabinet) for 24 h at room temperature. The micrographs were taken in the Advanced Laboratory of Electron Nanoscopy of CINVESTAV with a field emission scanning electron microscope (Zeiss Auriga-39-16) using the following parameters: Accelerating voltage, 2 kV; working distance, 3.8 nm; aperture, 7.5  $\mu$ m; and a secondary electron detector.

### *Animals*

Male BALB/c mice (body weight 20–25 g) were used and maintained in a Supermouse 1800 system (Lab Products, Inc.; Seaford, DE, USA) under 12-h light–dark cycles at a controlled temperature (20–22 °C) and humidity (55%) and free access to food and water. The experimental protocol was approved by the Institutional Animal Care and Use Committee of CINVESTAV (authorization no. 45109) certified by the Secretaría de Agricultura, Ganadería, Desarrollo Rural, Pesca y Alimentación (SAGARPA; NOM-062-ZOO-1999 and NOM-087-ECOL-

1995). The mice were habituated to the experimental room conditions for 1 week before the study.

All surgical and experimental procedures were performed in mice anesthetized with an intraperitoneal (i.p.) injection of an anesthesia mixture (ketamine, 120 mg – xylazine, 24 mg, per kg of body weight) in 0.9% of saline solution (Pisa Agropecuaria, Mexico).

#### Systemic administration

Three hundred microliters of NTS-polyplex NPs was injected into the retro-ophthalmic vein of anesthetized mice using insulin syringes (27G × 13 mm).<sup>14</sup>

#### GFP immunofluorescence

GFP expression was explored in the gastrointestinal tract, spleen, liver, kidney and heart using immunofluorescence on day 3 after an intravenous injection of NTS-polyplex NPs harboring the plasmid pEGFP-N1.<sup>6</sup> The transfected animals were anesthetized and then transcardially perfused with 50 mL of 0.01 M PBS (phosphate-buffered saline solution, pH 7.4) and 50 mL of 4% paraformaldehyde in PBS. The dissected organs were maintained in 0.01 M PBS containing 30% sucrose for 36 h at 4 °C and then sectioned into 30- $\mu$ m-thick slices using a sliding microtome (Leica SM2010 R, Leica Microsystem; Nussloch, Germany). For the immunostaining, the primary antibody was a rabbit polyclonal anti-GFP (1:1500; Abcam; Cambridge, MA, USA) and the secondary antibody was an Alexa Fluor 488 chicken anti-rabbit IgG (1:400; Molecular Probes Inc.; Eugene, OR). Tissue slices were mounted with Vectashield (Vector Laboratories; Burlingame CA) and examined using an epifluorescence Leica DMIRE2 microscope (Leica Microsystems; Nussloch, Germany). Alexa 488 fluorescence was detected at excitation-emission wavelengths of 488–522 nm, and the images were digitalized with a Leica DC300F camera (Leica Microsystems; Wetzlar, Germany).

#### NTS-polyplex NPs accumulation in reticuloendothelial tissues

BALB/c mice were intravenously injected with NTS-polyplex NPs previously labeled with propidium iodide as described elsewhere.<sup>2,4,14</sup> The animals were anesthetized and then transcardially perfused with 50 mL of 0.01 M PBS and 50 mL of 4% paraformaldehyde in PBS at 6 h and 48 h after injection. The lungs, kidneys, livers, and spleens were dissected, transferred to either 30% sucrose in 0.01 M PBS or formalin, serially sectioned into 8- $\mu$ m-thick slices using a cryostat (Leica CM1100, Leica; Heidelberg, Germany) and counterstained either with Hoechst 33258 (organs in sucrose) or hematoxylin and eosin (organs in formalin). The fluorescence was observed with a Leica DMIRE2 microscope (Leica Microsystem; Wetzlar, Germany) using a 20 $\times$  objective and the filters A for Hoechst 33258-nuclear staining (blue) and TX2 for propidium iodide (red). The images were digitalized with a Leica DC300F camera (Leica Microsystems; Nussloch, Germany) and processed using a Leica FW4000 fluorescence workstation, version V1.2.1 (Leica Microsystems Vertrieb GmbH; Bensheim, Germany). The hematoxylin-eosin stained sections were used for a histopathological examination.

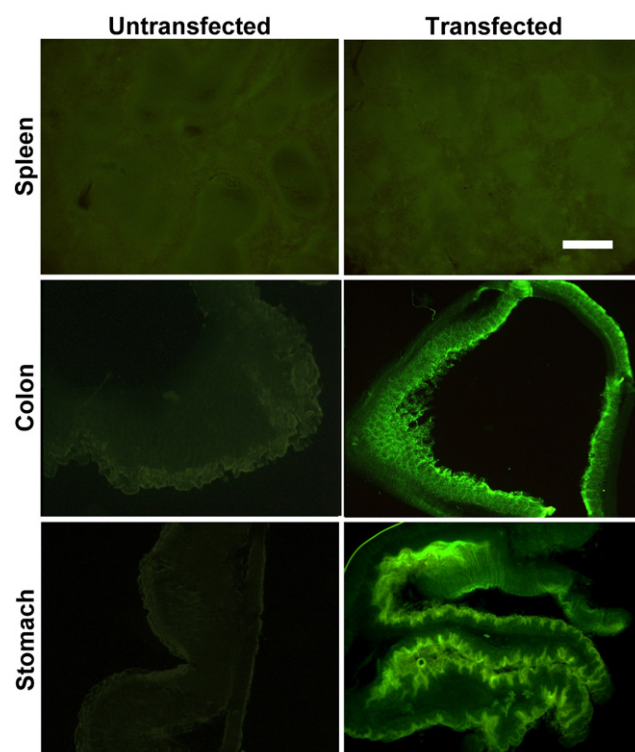


Figure 1. GFP expression in cells that constitutively express NTSR1. Representative micrographs of GFP-immunofluorescence on day 3 after an intravenous injection of NTS-polyplex NPs harboring the plasmid pEGFP-N1, which codes for the enhanced green fluorescent protein (GFP). The calibration bar = 1 mm and is common for all micrographs.

#### Blood collection and serum separation

The animals were anesthetized and 500  $\mu$ L of blood was then collected via cardiac puncture using insulin syringes (27G × 13 mm) at 0, 2, 4, 6 and 24 h (for measurements of proinflammatory cytokines) and at 24 and 96 h (for liver function tests, hematology profile and serum amyloid A (SAA) quantification) after treatment with sterile isotonic saline solution (SS), LPS, CCl<sub>4</sub> or NTS-polyplex ( $n$  = at least 5 mice in each time point for each experimental condition). The serum was separated using BD microtainer tubes with clot activator and gel (Becton Dickinson and Company; DF, MX), which were centrifuged at 1,000 g for 15 min at 4 °C. The blood specimens were collected in BD microtainers containing 1.0 mg of K<sub>2</sub>EDTA 24 h and 96 h after treatment with SS, LPS, CCl<sub>4</sub> or NTS-polyplex to test the hematology profile at the Laboratory of Hematology and Biochemistry, Pathology Department, School of Veterinary Medicine and Zootechnics, Autonomous University of Mexico (UNAM) using a hematology analyzer BC-2800 (Mindray Medical Mexico; DF, MX).

#### Liver function tests

Twenty-four and 96 h after a systemic injection of NTS-polyplex NPs, the serum levels of hepatic function markers were measured at the Laboratory of Hematology and Biochemistry,

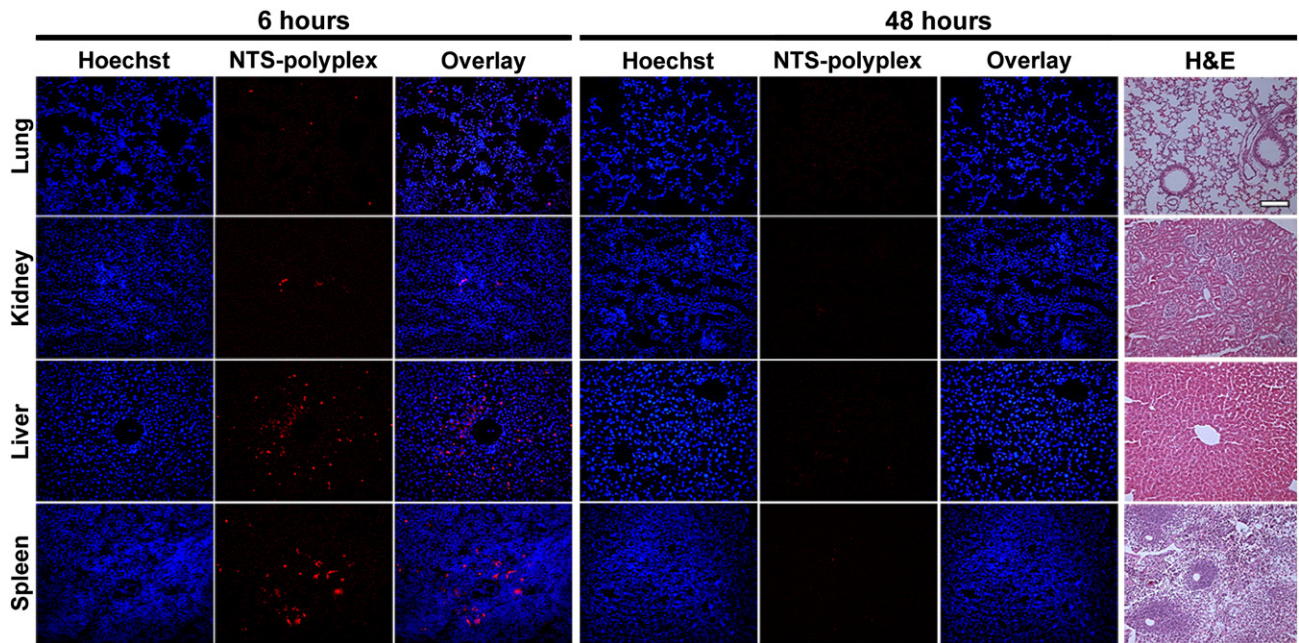


Figure 2. Biodistribution of propidium iodide-labeled pDNA after its delivery by NTS-polyplex NPs. Representative micrographs showing the fluorescence of propidium iodide and Hoechst 33258 at indicated times. Representative micrographs of hematoxylin-eosin stained sections taken at 48 h after the systemic transfection were included to show cytoarchitecture of the organs studied. The calibration bar = 50  $\mu\text{m}$  and is common for all micrographs.

Pathology Department, School of Veterinary Medicine and Zootechnics, UNAM. The aspartate aminotransferase (AST), alanine aminotransferase (ALT) and alkaline phosphatase (AP) levels were determined by spectrophotometry (Vital Scientific-Junior).<sup>31,32</sup> The total bilirubin and conjugated bilirubin levels were also measured.<sup>33</sup> An oral dose of  $\text{CCl}_4$  (150  $\mu\text{L}/150 \mu\text{L}$  of corn oil; Sigma-Aldrich; Saint Louis, MO, USA) and an i.p. injection of LPS (50  $\mu\text{g}/0.3 \text{ mL}$  of sterile 0.9% sodium chloride solution; Sigma-Aldrich; Saint Louis, MO, USA) were used as positive controls, whereas a systemic injection of SS was used as a negative control.

#### Serum levels of pro-inflammatory cytokines and serum amyloid A

The serum levels of proinflammatory cytokines were measured 0, 2, 4, 6 and 24 h after treatment with SS, LPS or NTS-polyplex. A multiplex immunobead assay (Milliplex MAP mouse Th17 magnetic Bead Panel) and a Luminex MAGPIX<sup>®</sup> detection System with xPONENT software (Millipore Corporation; Billerica, MA, USA) were used to measure the serum levels of IL-1 $\beta$ , IL-6 and TNF- $\alpha$  over time after various treatments. The standard curve for each pro-inflammatory cytokine was built with 6 standards, and the lower and upper limits of quantification (LLOQ and ULOQ) were calculated as the highest and lowest measured reliable standards for each standard curve. LLOQ refers to the amount of analyte that would provide a signal equal to the blank plus thrice the standard deviation of the blank. ULOQ is the point of saturation for an instrument detector at which higher amounts of analyte do not produce a linear response in the signal. The linear dynamic range (LDR) was defined as the lowest and highest standards on the linear part of each standard curve on a log–log plot. The LDR in pg/mL for

each analyte ranged from 14 to 15,000 for IL-1 $\beta$ , 7 to 8,647 for IL-6, and 3 to 3,006 for TNF- $\alpha$ .

The SAA level was determined 24 and 96 h after treatment with SS, LPS or NTS-polyplex using a solid phase enzyme-linked immune-sorbent assay (ELISA) kit that included a polyclonal anti-mouse SAA2 antibody as solid phase immobilization, a horseradish peroxidase (HRP) conjugated polyclonal anti-mouse SAA1/2 antibodies for detection, and a mouse serum of known SAA concentration for the standard curve (Life Diagnostics, PA, USA). The standard curve was plotted with optical density readings at 450 nm on the Y-axis against mouse SAA concentrations (8–500 ng/mL) on the X-axis.

#### Local inflammatory response assay

Local inflammation was produced by 30- $\mu\text{L}$  injections of 1% carrageenan (Cg) solution (a positive control), SS (a negative control) or NTS-polyplex NPs into the plantar pad of the left hind paws of BALB/c mice using a 1-mL syringe and a 27-gauge needle.<sup>34</sup> The width of the left and right hind paw, defined as the distance from the plantar to the dorsal surface at the paw center, was measured 1, 3, 5, and 24 h after the injection using a digital micrometer (measuring range from 0 to 0.5" with a resolution of 0.0005"; Tylertown, MS, USA). The results were expressed as the difference in the width ( $\Delta$  in mm) of the left and right hind paw of mouse. Upon completion of measurements, the mice were anesthetized to remove the hind paws at the level of the calcaneus bone for histopathological analysis and then beheaded.

#### Histopathology

After dissection, the lungs, kidneys, liver, spleen and hind paws were fixed in 10% neutral-buffered formalin and embedded

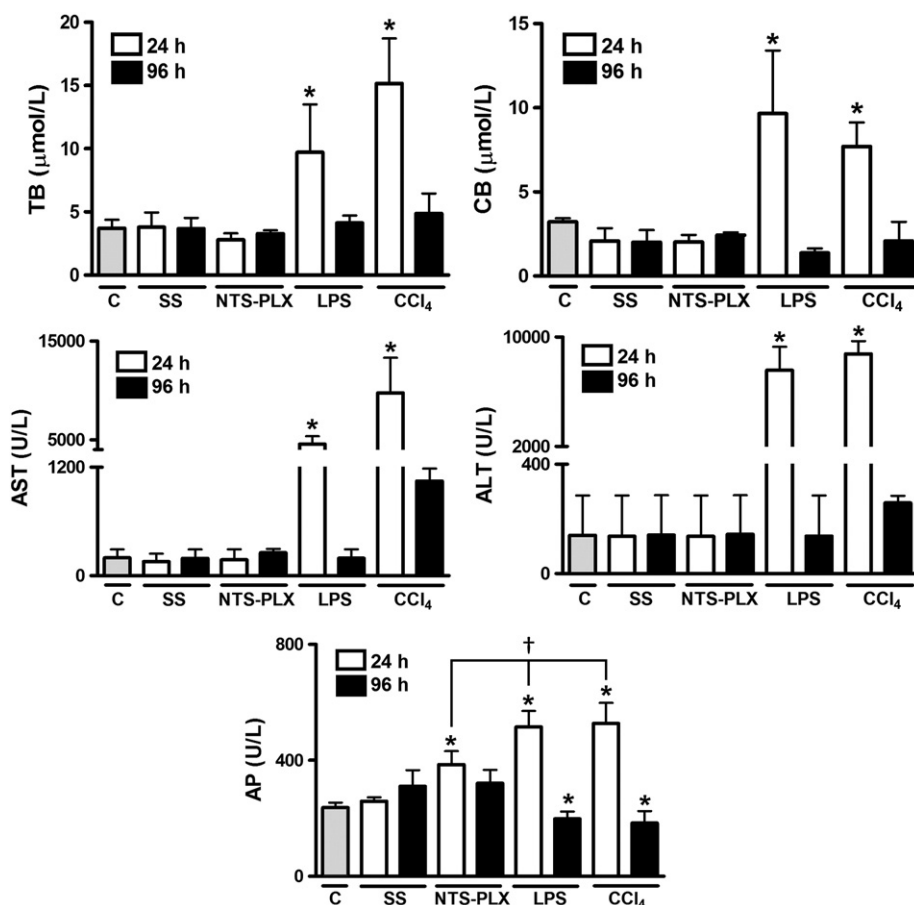


Figure 3. Liver function markers after various treatments. BALB/c mice treated with carbon tetrachloride (CCl<sub>4</sub>; 150 μL/150 μL corn oil) or lipopolysaccharide (LPS; 50 μg/0.3 mL in sterile saline solution) were used as positive controls. NTS-PLX refers to the group of mice treated with NTS-polyplex NPs harboring the plasmid pEGFP-N1. The negative control groups were untreated mice (C) and mice injected with sterile isotonic saline solution (SS). TB = total bilirubin; CB = conjugated bilirubin; AST = aspartate transaminase; ALT = alanine transaminase; AP = alkaline phosphatase. Values are mean ± σ of 5 independent experiments in each time evaluated. \**P* < 0.0001 to compare with the control group; †*P* < 0.001 to compared with the positive controls; a two-way ANOVA test and a post-hoc Bonferroni test.

in paraffin blocks. Serial 5-μm-thick sections were then cut with a cryostat-microtome model CM1100 (Leica Microsystems, Wetzlar, Germany), deparaffinized, and stained with hematoxylin and eosin for histopathological evaluation.

#### Statistical analysis

Values are provided as the mean ± standard deviation (σ) obtained from at least 5 independent experiments. After testing for normality with the Snedecor F-analysis, the significance of differences was analyzed by a two-way ANOVA test and a post-hoc Bonferroni test to compare the experimental with the control group using the Graph Pad Prism 5.0 (GradPad Software Inc., La Jolla, CA, USA). Statistical significance was established at *P* < 0.05.

## Results

#### Transgene expression

GFP expression was detected in the stomach and the intestinal tract cells (Figure 1) three days after the intravenous injection of

NTS-polyplex NPs formed at an optimal molar ratio (Figure S1). These cells are known to constitutively express NTSR1.<sup>23,24</sup> In contrast, GFP expression was not observed in the tissues where NTSR1 is absent,<sup>14</sup> such as the spleen (Figure 1), liver, lungs, kidneys and heart (data not shown).

#### NTS-polyplex NPs accumulation

To evaluate the possibility that large amounts of NTS-polyplex NPs could be incorporated in organs with mononuclear phagocyte system cells, a propidium iodide-labeled NTS-polyplex NPs was injected intravenously. Six hours after injection, the fluorescent label was found mainly in the liver and spleen, and in lesser amounts in the kidneys and lungs (Figure 2). Neither the fluorescent label nor morphological evidence of tissue damage was observed in these organs 48 h after injection (Figure 2). Therefore, these results suggest that the propidium iodide-labeled NTS-polyplex NPs are either cleared or filtered because mononuclear phagocyte system cells do not express NTSR1 and GFP expression was not detected (Figure 1).<sup>23,24</sup>

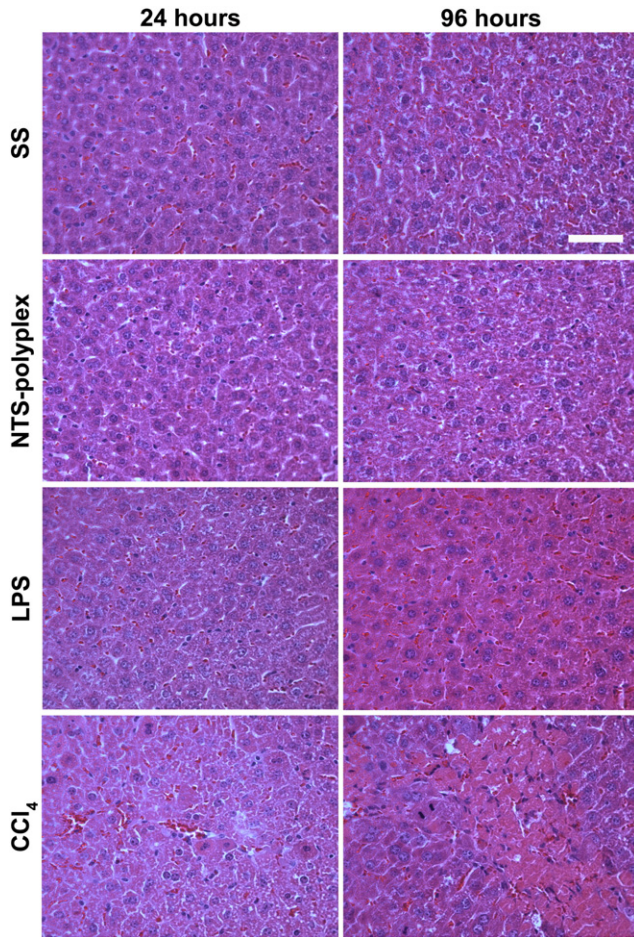


Figure 4. Representative microphotographs of liver sections stained with hematoxylin and eosin after different treatments. The negative control group was injected with sterile isotonic saline solution (SS). The positive controls were mice treated with carbon tetrachloride ( $\text{CCl}_4$ ; 150  $\mu\text{L}/50 \mu\text{L}$  corn oil) or lipopolysaccharide (LPS; 50  $\mu\text{g}/0.3 \text{ mL}$  in SS). BALB/c mice were treated with NTS-polyplex NPs at indicated times harboring the plasmid pEGFP-N1. Liver sections were 5- $\mu\text{m}$  in width and the calibration bar = 100  $\mu\text{m}$ .

#### Liver function evaluation

The liver is the organ that mainly participates in the clearance of foreign DNA in mice.<sup>17,35</sup> Consequently, the acute effects of the systemic injection of NTS-polyplex NPs on hepatic function were compared to those of negative controls (untreated mice and SS injection) and positive controls ( $\text{CCl}_4$  or LPS administration). The levels of total and conjugated bilirubin, AST, and ALT did not statistically differ between groups treated with NTS-polyplex NPs and the respective negative controls 24 h and 96 h after injection (Figure 3). Only the AP basal levels significantly increased by 63% at 24 h ( $386 \pm 46$ , U/L;  $P < 0.0001$ ) when compared with the negative controls, and these levels decreased ( $321 \pm 46$ , U/L) to values similar to the SS group ( $310 \pm 56$ , U/L) 96 h post-administration (Figure 3). However, the increase in AP levels produced by the NTS-polyplex NPs ( $386 \pm 46$ , U/L) was significantly lower than that induced by LPS ( $516 \pm 55$ , U/L;  $P < 0.001$ ) or  $\text{CCl}_4$  ( $528 \pm 71$ , U/L;  $P < 0.001$ ) 24 h post-administration.

The histopathological analysis of liver sections of negative controls showed a normal lobular organization that consisted of central veins and radially arranged hepatocytes with a mild vascular congestion (Figure 4). On the contrary, the positive controls LPS and  $\text{CCl}_4$  induced hepatic alterations, as expected.<sup>31,32,36</sup> After 24 h, LPS caused a major vascular and sinusoidal congestion as well as the diffusion of inflammatory cells and erythrocytes in hepatic sinusoids. An absence of nuclei, cariorrexis, disuse foci of necrotic parenchymal cells, cell swelling and congestion were observed after 96 h (Figure 4).  $\text{CCl}_4$  administration produced intense necrotic zones, edema, acute inflammatory infiltration, and hepatocyte degeneration characterized by cytoplasmic swelling and nuclear pyknosis 24 h post-administration and thereafter. The hepatic alterations were most severe 96 h after  $\text{CCl}_4$  administration (Figure 4). These changes were not detected in the hepatic architecture of mice transfected with NTS-polyplex NPs. Mild vascular congestion was observed in some zones, but the hepatic architecture was well preserved (Figure 4). In addition, histological alterations were not observed in the lungs, kidneys, and spleen after a systemic injection of NTS-polyplex NPs (Figure 2).

#### Systemic inflammatory response

The effect of an intravenous injection of NTS-polyplex NPs on the serum levels of pro-inflammatory cytokines was compared to that of SS (negative control) and LPS, a potent stimulant of the inflammatory response.<sup>37</sup> In the SS group, the levels of IL-1 $\beta$  and TNF- $\alpha$  remained stable during the experiment and were lower than the LDR (Figure 5). The levels of IL6 were within the LDR and varied from  $13 \pm 11 \text{ pg/mL}$  to  $50 \pm 44 \text{ pg/mL}$ , but significant differences were not found (Figure 5). Remarkably, the serum levels of the three pro-inflammatory cytokines in the group injected with NTS-polyplex NPs were similar to those of the respective negative controls at each evaluated time point (Figure 5). Compared with SS and NTS-polyplex NPs, LPS caused a drastic increase in the serum levels of IL-1 $\beta$  ( $25 \pm 9 \text{ pg/mL}$ ), IL-6 ( $9960 \pm 2150 \text{ pg/mL}$ ) and TNF- $\alpha$  ( $165 \pm 41 \text{ pg/mL}$ ) after 2 h. The levels subsequently progressively decreased and reached basal levels 24 h post-administration (Figure 5). As expected, high levels of SAA were detected 24 h ( $2200 \pm 182 \text{ ng/mL}$ ) and 96 h ( $2486 \pm 213 \text{ ng/mL}$ ) after LPS administration. Although the SAA levels increased in the NTS-polyplex NPs group ( $733 \pm 24 \text{ ng/mL}$ ) at 24 h, this increase was 2.8-fold lower than that induced by LPS and returned to the basal level ( $28 \pm 6 \text{ ng/mL}$ ) at 96 h (Figure 5).

The hematology profiles of the NTS-polyplex NPs group and positive controls were similar to that of the negative control (SS) at two time points evaluated in the current study (Table 1).

#### Local inflammatory response

To confirm the lack of an inflammatory effect, NTS-polyplex NPs were evaluated in a model of local inflammation using Cg as a positive control and SS as a negative control. A significant increase (450%) in the hind paw width was observed (Figure 6) as early as 1 h after Cg subcutaneous injection. Subsequently, this increase evolved over time and reached 1,556% 5 h post Cg injection, which suggested a strong inflammatory response

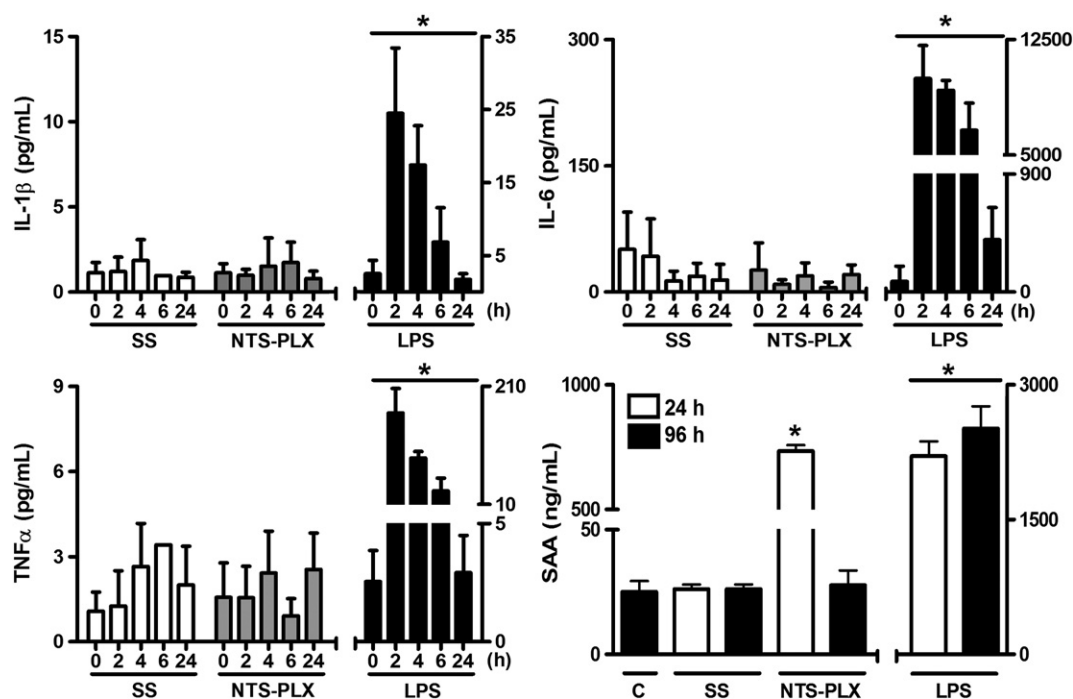


Figure 5. Serum levels of pro-inflammatory cytokines and serum amyloid A (SAA) after different treatments. SS = sterile isotonic saline solution, as a negative control. Lipopolysaccharide (LPS; 50  $\mu$ g/0.3 mL in SS). NTS-PLX = NTS-polyplex NPs harboring the plasmid pEGFP-N1. Each value is the mean  $\pm$   $\sigma$  of 5 (proinflammatory cytokines) or 6 (SAA) independent experiments in each time evaluated. \* $P$  < 0.01 a two-way ANOVA test and a post-hoc Bonferroni test to compare with the control group.

Table 1  
Comparison of hematologic profile.

Group	Htc L/L	Hb g/L	Erythrocytes $\times 10^{12}$ L	MCV f/L	MCHC g/L	Platelets $\times 10^9$ L	Leukocytes $\times 10^9$ L	Neutrophils $\times 10^9$ L	Monocytes $\times 10^9$ L	Lymphocytes $\times 10^9$ L	Eosinophils $\times 10^9$ L
Control	0.36 $\pm$ 0.02	110 $\pm$ 15	7.3 $\pm$ 1.07	47 $\pm$ 0.6	324 $\pm$ 0.6	238 $\pm$ 91	4.0 $\pm$ 0.9	0.98 $\pm$ 0.95	0.03 $\pm$ 0.06	2.9 $\pm$ 0.85	0.07 $\pm$ 0.06
SS											
24 h	0.37 $\pm$ 0.06	106 $\pm$ 19	7.3 $\pm$ 1.22	46 $\pm$ 1.5	323 $\pm$ 11	295 $\pm$ 52	3.7 $\pm$ 0	0.90 $\pm$ 0.35	0.07 $\pm$ 0.06	2.8 $\pm$ 0.07	0.10 $\pm$ 0
96 h	0.30 $\pm$ 0.07	107 $\pm$ 13	6.6 $\pm$ 1.5	46 $\pm$ 0.6	361.6 $\pm$ 58	336 $\pm$ 43	4.8 $\pm$ 0.07	1.4 $\pm$ 0.98	0.12 $\pm$ 0.07	2.9 $\pm$ 0.07	0.05 $\pm$ 0.5
PLX											
24 h	0.40 $\pm$ 0.1	133 $\pm$ 32	8.5 $\pm$ 1.99	47 $\pm$ 0.6	330 $\pm$ 5.6	315 $\pm$ 23	4.3 $\pm$ 0.8	0.97 $\pm$ 0.70	0.10 $\pm$ 0.00	2.2 $\pm$ 1.6	0
96 h	0.34 $\pm$ 0.4	123 $\pm$ 22	6.7 $\pm$ 1.9	45 $\pm$ 0.7	416.5 $\pm$ 54.4	320 $\pm$ 23	3.5 $\pm$ 2.2	0.75 $\pm$ 0.07	0.25 $\pm$ 0.03	2.2 $\pm$ 0.19	0.25 $\pm$ 0.35
LPS											
24 h	0.29 $\pm$ 0.06	93 $\pm$ 20	6.1 $\pm$ 1.27	46 $\pm$ 1.5	324 $\pm$ 11	260 $\pm$ 52	2.6 $\pm$ 1	0.83 $\pm$ 0.35	0.10 $\pm$ 0.00	2.4 $\pm$ 0.7	0
96 h	0.28 $\pm$ 0.07	88 $\pm$ 17	5.3 $\pm$ 0.85	46 $\pm$ 0.6	358 $\pm$ 48	312 $\pm$ 76	5.5 $\pm$ 0.35	1.4 $\pm$ 0.7	0.03 $\pm$ 0.0	3.2 $\pm$ 0.78	0.03 $\pm$ 0.06
CCl <sub>4</sub>											
24 h	0.49 $\pm$ 0.01	159 $\pm$ 5	10.4 $\pm$ 0.17	47 $\pm$ 0.5	327 $\pm$ 6	392 $\pm$ 13	6.7 $\pm$ 1.6	4.53 $\pm$ 2.47	0.24 $\pm$ 0.15	2.5 $\pm$ 0.5	0.03 $\pm$ 0.06
96 h	0.34 $\pm$ 0.08	114 $\pm$ 29	7.3 $\pm$ 1.7	46 $\pm$ 0.5	338 $\pm$ 11	394 $\pm$ 15	6.7 $\pm$ 0.37	2.7 $\pm$ 1.9	0.14 $\pm$ 0.0	4 $\pm$ 1.04	0

Values are mean  $\pm$  standard deviation ( $\sigma$ ) obtained from at least 5 independent experiments. The significance of differences was analyzed by a two-way ANOVA test and a post-hoc Bonferroni test to compare with the control group using the Graph Pad Prism 5.0 (GradPad Software Inc., La Jolla, CA, USA). The statistical significance was established at least  $P$  < 0.05. Abbreviations: Hematocrit (Htc), Hemoglobin (Hb), Mean Corpuscular Volume (MCV), Mean Corpuscular Hemoglobin Concentration (MCHC).

(Figure 6). On the contrary, the maximum effect of NTS-polyplex NPs subcutaneous injection was 43% at 1 h and subsequently decreased over time and reached control values (Figure 6). An injection of sterile SS produced a similar effect (Figure 6). The histopathology analysis of mouse paws 1 h after administration showed that SS or NTS-polyplex NPs resulted in subcutaneous edema without the infiltration of inflammatory

cells, whereas Cg caused a mild infiltration of inflammatory cells (data not shown). However, Cg induced marked inflammatory changes 5 h after injection, including pronounced cellular infiltration and mild disorganization of muscle fibers. On the contrary, neither SS nor NTS-polyplex NPs showed any histopathological alterations or inflammatory signs in the paw 5 h post-injection (Figure 6).

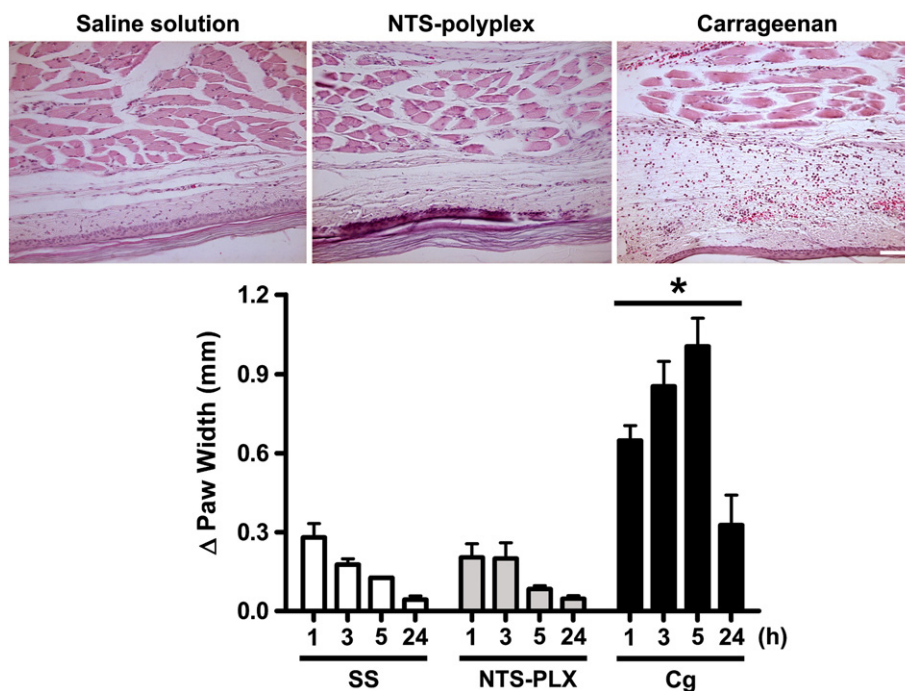


Figure 6. Time course of local inflammation after different subcutaneous treatments into the plantar hind paw of BALB/c mice. Thirty microliters of NTS-polyplex NPs harboring the plasmid pEGFP-N1 (NTS-PLX), 1% carrageenan solution (Cg; a positive control) or sterile isotonic saline solution (SS), as a negative control, was injected. Top panels are representative micrographs of hematoxylin-eosin stained sections taken at 5 h after the subcutaneous injection of the treatments as indicated. The graph shows the difference in the width ( $\Delta$  in mm) of the left and right hind paw of mouse. Each value is the mean  $\pm$   $\sigma$  of 12 independent experiments in each time evaluated. \* $P < 0.01$  a two-way ANOVA test and a post-hoc Bonferroni test to compare with the control group.

## Discussion

This study shows for the first time that targeted gene delivery to NTSR1-expressing cells of peripheral tissues by NTS-polyplex NPs does not produce an acute systemic inflammatory response or hepatic cytotoxicity. The lack of an inflammatory effect was confirmed by the injection of NTS-polyplex NPs in a mouse paw when compared to a Cg injection. These results are consistent with the notion that polyplexes have low toxicity and immunogenic potential<sup>25,26</sup> compared with lipopolyplexes and viral vectors.<sup>29</sup>

The presence of GFP expression in cells of the gastrointestinal tract, which are known to constitutively express NTSR1,<sup>23,24</sup> and the absence of GFP expression in other tissues that lack these receptors (liver, lung, spleen, kidney and heart) support the mediation of NTSR1 in the transfection by NTS-polyplex NPs as previously shown in cell culture<sup>3-5</sup> and experimental animal<sup>1,4,6,14</sup> studies. However, recent evidence shows that normal B lymphocytes, one of the resident cells in the spleen, express functional NTSR1.<sup>38</sup> Therefore, the presence of propidium iodide-labeled NTS-polyplex NPs in the spleen 6 h and 48 h after injection suggests that certain cell populations might be transfected. However, GFP expression, which was evaluated 3 days after NTS-polyplex injection, was not observed. This lack of expression might be attributed to the migration of B cells in the spleen at this time. Alternatively, the NTS-polyplex NPs could accumulate in the liver and spleen for clearance because the liver and spleen are the main organs that participate in the clearance of other polyplex NP systems by phagocytic

uptake and filtration.<sup>17,22,39</sup> An excessive accumulation of NPs in these organs could potentially elicit a strong inflammatory response and eventually lead to cell death, which is usually manifested by increased levels of biochemical markers in the serum. In contrast to LPS and CCl<sub>4</sub> (positive controls), the systemic administration of NTS-polyplex NPs did not alter the serum levels of liver function markers, which suggests that NTS-polyplex NPs accumulation did not reach the levels necessary to elicit severe hepatic inflammation. These results are also consistent with the outcome of our histopathological studies. Nevertheless, the GFP transgene would not necessarily cause damage, but a transgene that induces apoptosis used as an antineoplastic tool could cause a deleterious effect not only in the cancer cells but also in the specifically transfected tissues that constitutively express NTSR1.<sup>23,24</sup> In the case of neurotrophic therapy for Parkinson disease, the uncontrolled and robust expression of a neurotrophic protein might lead to undesirable side effects, such as aberrant innervation of the regenerating dopaminergic fibers and decreased dopamine synthesis.<sup>7</sup> Furthermore, neurotrophins, for instance, could reach sufficiently high levels to stimulate the p75 receptor, which leads to the apoptosis of healthy and recovering neurons.<sup>7</sup> Inducible promoters can be used in conjunction with NTS-polyplex to restrain the transgene expression and avoid undesirable side effects.

IL-1 $\beta$ , IL-6 and TNF- $\alpha$  are the most notable pro-inflammatory cytokines secreted by local neutrophil granulocytes and macrophages into the bloodstream during an acute inflammatory process.<sup>40-42</sup> Accordingly, LPS (positive control in this study) increased the serum levels of these three pro-inflammatory

cytokines as previously reported.<sup>43,44</sup> On the contrary, the serum levels of IL-1 $\beta$ , IL-6 and TNF- $\alpha$  were similar to that of the negative control (SS injection) after a systemic injection of NTS-polyplex NPs, which supports their lack of pro-inflammatory effect. These results agree with the failure of a systemic injection of DNA- or siRNA-linear polyethylenimine nanoparticles to increase TNF- $\alpha$  serum levels and hepatic enzymes.<sup>26,45</sup>

Thus, a rapid escape of polyplex NPs from the endosome might be a crucial factor to avoid the activation of toll-like receptor 9 (TLR9) and consequently the activation of NF- $\kappa$ B.<sup>25</sup> This aspect could explain the lack of inflammatory effects of polyethyleneimine-based polyplexes<sup>25,26,45</sup> and fusogenic peptide-carrying NTS-polyplex NPs, which enables their rapid escape from endosome.<sup>4,6</sup> This mechanism allows the foreign DNA to bypass lysosomal degradation. This bypass avoids the exposition of unmethylated CpG motifs,<sup>26,45,46</sup> which are recognized by TLR9 to cause inflammation in experimental animals.<sup>47</sup> Another advantage of polyplex NPs might be the efficient compaction of foreign DNA that might conceal CpG motifs in contrast to lipoplexes that are more immunogenic exposing CpG motifs.<sup>29,48</sup> Despite the lack of pro-inflammatory effect of systemically or locally injected NTS-polyplex NPs, a minor and reversible increase was determined in the AP and SAA levels when compared with the LPS effect. IL-1 $\beta$ , IL-6 and TNF- $\alpha$  have long been known to stimulate SAA production during acute inflammation.<sup>49,50</sup> Therefore, the reversible SAA accumulation observed 24 h after NTS-polyplex NP injection might have led to a minor and reversible liver injury in the absence of increased serum IL-1 $\beta$ , IL-6 and TNF- $\alpha$  levels. However, this possibility was not detected in the histopathological analysis.

In summary, major histopathological alterations or increases in the serum levels of IL-1 $\beta$ , IL-6, TNF- $\alpha$ , bilirubin, AST and ALT were not detected after a systemic delivery of NTS-polyplex NPs. The transient increase in the serum levels of AP and SAA in the absence of IL-1 $\beta$ , IL-6, and TNF- $\alpha$  production might have been induced by a transient osmotic shock in the liver caused by NTS-polyplex NPs accumulation. Moreover, minor reversible edema without inflammation was observed in the mouse paw after a local injection of NTS-polyplex NPs. Thus, these results indicate that NTS-polyplex NPs can specifically transfect NTSR1-expressing cells without stimulating the acute inflammatory response. Nevertheless, the ability of NTS-polyplex NPs to evoke the innate and adaptive immune response should be further evaluated in appropriate models of neurotrophic factor gene therapy and suicide gene therapy using immunocompetent animals before their application in clinical trials of gene therapy for Parkinson's disease and cancers of cells expressing NTSR1.<sup>7,13</sup>

## Acknowledgments

We thank Josué Romero Ibarra, LANE, for the support of the NTS-polyplex NPs analysis by field emission scanning electron microscopy and Ricardo Gaxiola Centeno, UPEAL, for the care and management of animals, CINVESTAV. We also thank Arlette Castillo Mata, Lab. Bioquímica Clínica, for the determination of liver markers and Luis Enrique García Ortuño,

Laboratorio de Patología Clínica, for the determination of hematology profile, Departamento de Patología, FMVZ-UNAM.

## Appendix A. Supplementary data

Supplementary data to this article can be found online at <http://dx.doi.org/10.1016/j.nano.2013.11.013>.

## References

- Alvarez-Maya I, Navarro-Quiroga I, Meraz-Rios MA, Aceves J, Martinez-Fong D. In vivo gene transfer to dopamine neurons of rat substantia nigra via the high-affinity neurotensin receptor. *Mol Med* 2001;**7**:186-92.
- Martinez-Fong D, Navarro-Quiroga I. Synthesis of a non-viral vector for gene transfer via the high-affinity neurotensin receptor. *Brain Res Brain Res Protoc* 2000;**6**:13-24.
- Martinez-Fong D, Navarro-Quiroga I, Ochoa I, Alvarez-Maya I, Meraz MA, Luna J, et al. Neurotensin-SPDP-poly-L-lysine conjugate: a nonviral vector for targeted gene delivery to neural cells. *Brain Res Mol Brain Res* 1999;**69**:249-62.
- Navarro-Quiroga I, Antonio Gonzalez-Barrios J, Barron-Moreno F, Gonzalez-Bernal V, Martinez-Arguelles DB, Martinez-Fong D. Improved neurotensin-vector-mediated gene transfer by the coupling of hemagglutinin HA2 fusogenic peptide and Vp1 SV40 nuclear localization signal. *Brain Res Mol Brain Res* 2002;**105**:86-97.
- Hernandez-Baltazar D, Martinez-Fong D, Trudeau LE. Optimizing NTS-polyplex as a tool for gene transfer to cultured dopamine neurons. *PLoS One* 2012;**7**:e51341.
- Arango-Rodriguez ML, Navarro-Quiroga I, Gonzalez-Barrios JA, Martinez-Arguelles DB, Bannon MJ, Kouri J, et al. Biophysical characteristics of neurotensin polyplex for in vitro and in vivo gene transfection. *Biochim Biophys Acta* 2006;**1760**:1009-20.
- Martinez-Fong D, Bannon MJ, Trudeau LE, Gonzalez-Barrios JA, Arango-Rodriguez ML, Hernandez-Chan NG, et al. NTS-Polyplex: a potential nanocarrier for neurotrophic therapy of Parkinson's disease. *Nanomedicine* 2012;**8**:1052-69.
- Gonzalez-Barrios JA, Lindahl M, Bannon MJ, Anaya-Martinez V, Flores G, Navarro-Quiroga I, et al. Neurotensin polyplex as an efficient carrier for delivering the human GDNF gene into nigral dopamine neurons of hemiparkinsonian rats. *Mol Ther* 2006;**14**:857-65.
- Sadoul JL, Checler F, Kitabgi P, Rostene W, Javoy-Agid F, Vincent JP. Loss of high affinity neurotensin receptors in substantia nigra from parkinsonian subjects. *Biochem Biophys Res Commun* 1984;**125**:395-404.
- Szigethy E, Beaudet A. Correspondence between high affinity 125I-neurotensin binding sites and dopaminergic neurons in the rat substantia nigra and ventral tegmental area: a combined radioautographic and immunohistochemical light microscopic study. *J Comp Neurol* 1989;**279**:128-37.
- Souaze F, Viardot-Foucault V, Roulet N, Toy-Miou-Leong M, Gompel A, Bruyneel E, et al. Neurotensin receptor 1 gene activation by the Tcf/ $\beta$ -catenin pathway is an early event in human colonic adenomas. *Carcinogenesis* 2006;**27**:708-16.
- Dupouy S, Mourra N, Doan VK, Gompel A, Alifano M, Forgez P. The potential use of the neurotensin high affinity receptor 1 as a biomarker for cancer progression and as a component of personalized medicine in selective cancers. *Biochimie* 2011;**93**:1369-78.
- Wu Z, Martinez-Fong D, Tredaniel J, Forgez P. Neurotensin and its high affinity receptor 1 as a potential pharmacological target in cancer therapy. *Front Endocrinol (Lausanne)* 2012;**3**:184.
- Rubio-Zapata HA, Rembao-Bojorquez JD, Arango-Rodriguez ML, Dupouy S, Forgez P, Martinez-Fong D. NT-polyplex: a new tool for

- therapeutic gene delivery to neuroblastoma tumors. *Cancer Gene Ther* 2009;**16**:573-84.
15. Castillo-Rodriguez R, Arango-Rodriguez M, Escobedo L, Rubio-Zapata H, Tellez-Lopez V, Mejia-Castillo T, et al. Neurotensin-Polyplex as a Potential Tool in Gene Therapy for Human Breast Cancer. *Eur J Cancer* 2012;**48**:S93.
  16. Nie S. Understanding and overcoming major barriers in cancer nanomedicine. *Nanomedicine (Lond)* 2010;**5**:523-8.
  17. Ward CM, Read ML, Seymour LW. Systemic circulation of poly(L-lysine)/DNA vectors is influenced by polycation molecular weight and type of DNA: differential circulation in mice and rats and the implications for human gene therapy. *Blood* 2001;**97**:2221-9.
  18. Neun BW, Dobrovolskaia MA. Method for analysis of nanoparticle hemolytic properties in vitro. *Methods Mol Biol* 2011;**697**:215-24.
  19. Verbaan FJ, Oussoren C, van Dam IM, Takakura Y, Hashida M, Crommelin DJ, et al. The fate of poly(2-dimethyl amino ethyl) methacrylate-based polyplexes after intravenous administration. *Int J Pharm* 2001;**214**:99-101.
  20. Pack DW, Hoffman AS, Pun S, Stayton PS. Design and development of polymers for gene delivery. *Nat Rev Drug Discov* 2005;**4**:581-93.
  21. Owens 3rd DE, Peppas NA. Opsonization, biodistribution, and pharmacokinetics of polymeric nanoparticles. *Int J Pharm* 2006;**307**:93-102.
  22. Alexis F, Pridgen E, Molnar LK, Farokhzad OC. Factors affecting the clearance and biodistribution of polymeric nanoparticles. *Mol Pharm* 2008;**5**:505-15.
  23. Mendez M, Souza F, Nagano M, Kelly PA, Rostene W, Forgez P. High affinity neurotensin receptor mRNA distribution in rat brain and peripheral tissues. Analysis by quantitative RT-PCR. *J Mol Neurosci* 1997;**9**:93-102.
  24. Carraway R, Leeman SE. Characterization of radioimmunoassayable neurotensin in the rat. Its differential distribution in the central nervous system, small intestine, and stomach. *J Biol Chem* 1976;**251**:7045-52.
  25. Saito Y, Higuchi Y, Kawakami S, Yamashita F, Hashida M. Immunostimulatory characteristics induced by linear polyethylenimine-plasmid DNA complexes in cultured macrophages. *Hum Gene Ther* 2009;**20**:137-45.
  26. Kawakami S, Ito Y, Charoensit P, Yamashita F, Hashida M. Evaluation of proinflammatory cytokine production induced by linear and branched polyethylenimine/plasmid DNA complexes in mice. *J Pharmacol Exp Ther* 2006;**317**:1382-90.
  27. Plank C, Mechtler K, Szoka Jr FC, Wagner E. Activation of the complement system by synthetic DNA complexes: a potential barrier for intravenous gene delivery. *Hum Gene Ther* 1996;**7**:1437-46.
  28. Higashisaka K, Yoshioka Y, Yamashita K, Morishita Y, Fujimura M, Nabeshi H, et al. Acute phase proteins as biomarkers for predicting the exposure and toxicity of nanomaterials. *Biomaterials* 2011;**32**:3-9.
  29. Sakurai H, Kawabata K, Sakurai F, Nakagawa S, Mizuguchi H. Innate immune response induced by gene delivery vectors. *Int J Pharm* 2008;**354**:9-15.
  30. Zhu J, Huang X, Yang Y. The TLR9-MyD88 pathway is critical for adaptive immune responses to adeno-associated virus gene therapy vectors in mice. *J Clin Invest* 2009;**119**:2388-98.
  31. Sotelo-Felix JI, Martinez-Fong D, Muriel De la Torre P. Protective effect of carnosol on CCl(4)-induced acute liver damage in rats. *Eur J Gastroenterol Hepatol* 2002;**14**:1001-6.
  32. Sotelo-Felix JI, Martinez-Fong D, Muriel P, Santillan RL, Castillo D, Yahuaca P. Evaluation of the effectiveness of Rosmarinus officinalis (Lamiaceae) in the alleviation of carbon tetrachloride-induced acute hepatotoxicity in the rat. *J Ethnopharmacol* 2002;**81**:145-54.
  33. Winsten S, Cehelyk B. A rapid micro diazo technique for measuring total bilirubin. *Clin Chim Acta* 1969;**25**:441-6.
  34. Morris CJ. Carrageenan-induced paw edema in the rat and mouse. *Methods Mol Biol* 2003;**225**:115-21.
  35. Liu F, Shollenberger LM, Conwell CC, Yuan X, Huang L. Mechanism of naked DNA clearance after intravenous injection. *J Gene Med* 2007;**9**:613-9.
  36. Yuan H, Li L, Zheng W, Wan J, Ge P, Li H, et al. Antidiabetic drug metformin alleviates endotoxin-induced fulminant liver injury in mice. *Int Immunopharmacol* 2012;**12**:682-8.
  37. Morris M, Li L. Molecular mechanisms and pathological consequences of endotoxin tolerance and priming. *Arch Immunol Ther Exp (Warsz)* 2012;**60**:13-8.
  38. Saada S, Marget P, Fauchais AL, Lise MC, Chemin G, Sindou P, et al. Differential expression of neurotensin and specific receptors, NTSR1 and NTSR2, in normal and malignant human B lymphocytes. *J Immunol* 2012;**189**:5293-303.
  39. Merkel OM, Librizzi D, Pfestroff A, Schurrat T, Buyens K, Sanders NN, et al. Stability of siRNA polyplexes from poly(ethylenimine) and poly(ethylenimine)-g-poly(ethylene glycol) under in vivo conditions: effects on pharmacokinetics and biodistribution measured by Fluorescence Fluctuation Spectroscopy and Single Photon Emission Computed Tomography (SPECT) imaging. *J Control Release* 2009;**138**:148-59.
  40. Negash AA, Ramos HJ, Crochet N, Lau DT, Doehle B, Papic N, et al. IL-1beta production through the NLRP3 inflammasome by hepatic macrophages links hepatitis C virus infection with liver inflammation and disease. *PLoS Pathog* 2013;**9**:e1003330.
  41. Rose-John S. IL-6 trans-signaling via the soluble IL-6 receptor: importance for the pro-inflammatory activities of IL-6. *Int J Biol Sci* 2012;**8**:1237-47.
  42. He C, Yin L, Tang C, Yin C. Multifunctional polymeric nanoparticles for oral delivery of TNF-alpha siRNA to macrophages. *Biomaterials* 2013;**34**:2843-54.
  43. Erickson MA, Banks WA. Cytokine and chemokine responses in serum and brain after single and repeated injections of lipopolysaccharide: multiplex quantification with path analysis. *Brain Behav Immun* 2011;**25**:1637-48.
  44. Spinelle-Jaegle S, Devillier P, Doucet S, Millet S, Banissi C, Diu-Hercend A, et al. Inflammatory cytokine production in interferon-gamma-primed mice, challenged with lipopolysaccharide. Inhibition by SK&F 86002 and interleukin-1 beta-converting enzyme inhibitor. *Eur Cytokine Netw* 2001;**12**:280-9.
  45. Bonnet ME, Erbacher P, Bolcato-Bellemin AL. Systemic delivery of DNA or siRNA mediated by linear polyethylenimine (L-PEI) does not induce an inflammatory response. *Pharm Res* 2008;**25**:2972-82.
  46. Yew NS, Zhao H, Wu IH, Song A, Tousignant JD, Przybylska M, et al. Reduced inflammatory response to plasmid DNA vectors by elimination and inhibition of immunostimulatory CpG motifs. *Mol Ther* 2000;**1**:255-62.
  47. Knuefermann P, Baumgarten G, Koch A, Schwederski M, Velten M, Ehrentraut H, et al. CpG oligonucleotide activates Toll-like receptor 9 and causes lung inflammation in vivo. *Respir Res* 2007;**8**:72.
  48. Zhao H, Hemmi H, Akira S, Cheng SH, Scheule RK, Yew NS. Contribution of Toll-like receptor 9 signaling to the acute inflammatory response to nonviral vectors. *Mol Ther* 2004;**9**:241-8.
  49. Kisilevsky R, Manley PN. Acute-phase serum amyloid A: perspectives on its physiological and pathological roles. *Amyloid* 2012;**19**:5-14.
  50. Ghezzi P, Sipe JD. Dexamethasone modulation of LPS, IL-1, and TNF stimulated serum amyloid A synthesis in mice. *Lymphokine Res* 1988;**7**:157-66.